

Thermal conductivity of one-dimensional Fibonacci quasicrystals

Enrique Maciá*

GISC, Departamento de Física de Materiales, Facultad de Físicas, Universidad Complutense, E-28040 Madrid, Spain

(Received 11 February 1999; revised manuscript received 8 October 1999)

We consider a general Fibonacci quasicrystal (FQC) in which both the masses and the elastic constants are aperiodically arranged. Making use of a suitable decimation scheme, inspired by real-space renormalization-group concepts, we obtain closed analytical expressions for the global transfer matrix and transmission coefficient for several resonant critical normal modes. The fractal structure of the frequency spectrum significantly influences both the cumulative contribution of the different normal modes to the thermal transport and the dependence of the thermal conductivity with the temperature over a wide temperature range. The role of resonant effects in the heat transport through the FQC is numerically and analytically discussed.

I. INTRODUCTION

The discovery of thermodynamically stable quasicrystalline alloys of high structural quality in icosahedral¹ and decagonal² systems has opened promising avenues in the study of the physical properties of quasicrystals (QCs),^{3,4} allowing for detailed experimental studies of their related transport properties.

The thermal conductivity $\kappa(T)$ of several QC samples, covering different temperature ranges, has been measured, and the following general conclusions can be drawn from the collected data. In the first place, the heat transport is unusually low. For example, in AlPdMn icosahedral phases the thermal conductivity at room temperature is comparable to that of zirconia ($1 \text{ W m}^{-1} \text{ K}^{-1}$), and this value decreases to about $10^{-4} \text{ W m}^{-1} \text{ K}^{-1}$ below 0.1 K.⁵ In the second place, the contribution of electrons to the thermal transport is, at least, one order of magnitude lower than that due to phonons over a wide temperature range ($0.1 \text{ K} \leq T \leq 200 \text{ K}$).⁶ In the third place, the overall behavior of the thermal conductivity is quite sensitive to the microstructure of the sample. Thus, for polygrained samples, the lattice thermal conductivity monotonically increases with T , showing a marked tendency to saturation for temperatures above 10–20 K, and exhibiting a characteristic plateau extending from about 25 to 55 K.⁷ On the contrary, the lattice thermal conductivity of single-grained samples first increases with increasing T , it reaches a shallow maximum at about 20 K, and then smoothly decreases with further increasing T .^{7,8}

At first glance, it would be tempting to say that the thermal behavior of polygrained QCs is similar to that observed in amorphous materials; meanwhile the thermal conductivity curve of single-grained QCs resembles that observed in crystalline materials. However, a closer scrutiny of the obtained experimental curves reveals the existence of significant quantitative differences. In fact, the thermal conductivity of most amorphous materials is characterized by two main features: (a) Below 1 K the thermal conductivity can be fitted by a power law $\kappa = AT^\delta$, with $1.8 \leq \delta \leq 2.0$, and (b) around 10 K one finds a plateau exhibiting a constant value $\kappa \approx 0.1\text{--}0.2 \text{ W m}^{-1} \text{ K}^{-1}$.⁹ Keeping these facts in mind, we realize that, in polygrained QCs, the plateau occurs at substantially higher temperatures than those typically observed

for amorphous solids. Furthermore, in the low-temperature regime the thermal conductivity drops below the corresponding amorphous value, obeying a power law given by an exponent $\delta \approx 2.5$.⁶ In addition, the thermal conductivity curve of single-grained QCs exhibits a well-defined maximum at about 20 K, but this maximum is followed by a shallow minimum, located between 50 and 90 K, which is not observed in the usual crystalline samples.^{7,10}

Consequently, experimental results indicate the existence of both common features and significant differences in the thermal conductivity among polygrained QCs and amorphous solids, on the one hand, and single-grained QCs and crystalline solids, on the other hand. From a theoretical point of view the fundamental question concerning whether the purported anomalies in QC transport properties should be mainly attributed (or not) to the characteristic *quasiperiodic order* of their structure is still awaiting a definitive answer. Thus, it has been argued that the thermal conductivity behavior observed in polygrained QCs at the low-temperature range ($0.35 \text{ K} \leq T \leq 1.6 \text{ K}$), may be attributed to the phonon scattering by tunneling states, whose possible existence in AlPdMn QCs has been recently claimed from ultrasound experiments.¹¹ On the other hand, in the regime of intermediate temperatures, the plateau-type feature in the lattice thermal conductivity has been justified by invoking a generalization of the umklapp process to describe the scattering among phonons and the quasilattice structure.¹⁰ Finally, at higher temperatures, a phonon-assisted hopping mechanism has been proposed to act over hierarchically distributed hopping distances.¹² However, a general consensus on the relative importance of the different proposed mechanisms, as well as on their respective range of applicability, is still missing.

In this work, we will propose a general Fibonacci QC (FQC) in order to investigate the influence of the singular phonon spectrum structure on the thermal properties of one-dimensional (1D) quasiperiodic systems. In this way, we complement some of the few results previously obtained on the subject,¹³ providing substantial support to the thermodynamical implications associated with the peculiar nature of fractal energy spectra.¹⁴ To this end, we first discuss the major features of our general model as compared to previous models considered in the literature. Afterward, we report on

the general structure of the frequency spectrum, showing that its overall fragmentation scheme can be properly described in terms of resonant coupling effects. Next, we consider the physical nature of the phonon states, reporting on the richness of the physical behaviors exhibited by the different kinds of critical normal modes present in the quasilattice. Then, we study the contribution of the different normal modes to the thermal energy transport, and report on the presence of resonant effects in the thermal coefficient behavior. Finally, we consider the temperature dependence of the thermal conductivity curve, and compare the obtained curves with suitable experimental results of high-quality quasicrystalline samples.

II. MODEL

In our study we consider a harmonic chain composed of two kinds of masses, m_A and m_B , which are arranged according to the Fibonacci sequence, and two kinds of springs, K_{AA} and $K_{AB} = K_{BA}$, depending on the type of joined atoms. In this way, the quasiperiodic distribution of masses in the system induces an aperiodic (non-Fibonacci) distribution of spring constants in the chain. This characteristic feature is physically sound since, generally speaking, one expects that the nature of the chemical bonding between the different atoms (and thereof the value of the spring constant representing the bond) will depend on the nature of the involved atoms. In this sense, our FQC model is both more *general* and *simpler* than most of the systems previously discussed in the literature.^{15–21}

Making use of the transfer-matrix formalism the equation of motion can be cast in the form

$$\begin{pmatrix} u_{n+1} \\ u_n \end{pmatrix} = \begin{pmatrix} \frac{a_n}{K_{n,n+1}} & -\frac{K_{n,n-1}}{K_{n,n+1}} \\ 1 & 0 \end{pmatrix} \begin{pmatrix} u_n \\ u_{n-1} \end{pmatrix} \equiv P_n \begin{pmatrix} u_n \\ u_{n-1} \end{pmatrix}, \quad (1)$$

where u_n is the displacement of the n th atom from its equilibrium position; m_n , with $n=A,B$, is the corresponding mass, $K_{n,n\pm 1}$ denotes the strength of the harmonic coupling between neighbor atoms, ω is the vibration frequency, and $a_n \equiv K_{n,n-1} + K_{n,n+1} - m_n \omega^2$. The allowed regions of the frequency spectrum are determined from the usual spectral condition²² $|\text{Tr} M(N, \omega)| \equiv |\text{Tr}(\prod_{n=1}^N P_n)| \leq 2$, where $M(N, \omega)$ is the global transfer matrix, and $N = F_n$ is the number of atoms in the chain, where F_n is a Fibonacci number obtained from the recursive law $F_n = F_{n-1} + F_{n-2}$, with $F_0 = F_1 = 1$. From knowledge of the global transfer-matrix elements M_{ij} , we can obtain the transmission, $t(N, \omega)$, and Lyapunov, $\Gamma(N, \omega)$, coefficients through the standard expressions $t(N, \omega) = 4 \sin^2 k / \mathcal{D}(N, \omega)$, with

$$\mathcal{D} \equiv [M_{12} - M_{21} + (M_{11} - M_{22}) \cos k]^2 + (M_{11} + M_{22})^2 \sin^2 k, \quad (2)$$

where $\cos k = 1 - m_A \omega^2 / 2K_{AA}$ gives the dispersion relation for a periodic chain composed of A sites, and

$$\Gamma(N, \omega) = \frac{1}{N} \ln(M_{11}^2 + M_{12}^2 + M_{21}^2 + M_{22}^2). \quad (3)$$

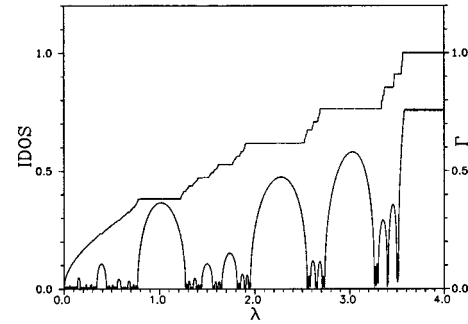


FIG. 1. Overall structure of the frequency spectrum for a Fibonacci quasicrystal with $N=610$, $\alpha=2$, and $\gamma=1.2$, as given by the IDOS and the Lyapunov coefficient.

Finally, we will evaluate the integrated density of states (IDOS) by node counting.²³

III. FREQUENCY SPECTRUM

We have studied in detail different realizations of the FQC by varying the number of constituent atoms, N , their mass ratio $\alpha \equiv m_B/m_A$, and the spring constants ratio $\gamma \equiv K_{AA}/K_{AB}$. Without loss of generality we have fixed $m_A \equiv 1$ and $K_{AB} \equiv 1$ as reference values, and have explored the parameter space within the intervals $34 \leq N \leq 1597$, $1 \leq \alpha \leq 5$, and $0.5 \leq \gamma \leq 3$. The overall structure of the frequency spectrum corresponding to the FQC is illustrated in Figs. 1 and 2 in terms of the parametrized frequency $\lambda \equiv m_A \omega^2 / K_{AB} = \omega^2$. From these figures we can draw the following conclusions: (i) The frequency spectrum shows a pentafurcation scheme, characterized by the presence of five main subbands separated by well-defined gaps. Therefore, the overall structure of the FQC phonon spectrum differs from those observed both for transfer models (three main subbands) and on-site models (four main subbands). (ii) At low and intermediate frequencies ($0 \leq \lambda \leq 2$), the minima of the Lyapunov coefficient take significantly low values. Conversely, starting about $\lambda = 2$ we realize that these minima monotonically increase with λ . Such a behavior suggests that the high-frequency phonons are more localized than the low-frequency ones. (iii) Most of the low-frequency phonons exhibit transmission coefficients close to unity. On the contrary, starting about $\lambda \sim 1.5$, we observe that, as the phonon frequency increases, the values of the corresponding transmission coefficients progressively decrease. Nevertheless,

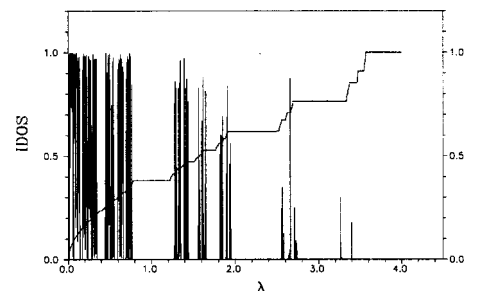


FIG. 2. Overall structure of the frequency spectrum for a Fibonacci quasicrystal with $N=610$, $\alpha=2$, and $\gamma=1.2$, as given by the IDOS and the transmission coefficient.

superimposed onto this general trend, we also find a few high-frequency phonon states exhibiting transmission coefficients significantly close to unity. We will study some of these states in more detail in Sec. IV.

We have confirmed that the overall structure of the frequency spectrum, as determined by the three features just described, does not significantly depend on the values adopted for the different model parameters. In addition, we have measured the heights of the characteristic steps appearing in the IDOS for a wide range of N , α , and γ parameters. The measured heights yield the same values for all the model parameters considered. These values agree within an error less than 0.1% with the series $\tau^3:\tau^4:\tau^3:\tau^4:\tau^3$, ordered according to growing frequencies, where $\tau=(\sqrt{5}-1)/2$ is the inverse golden mean. This result agrees well with the gap labeling theorem which states that at any gap of the energy spectrum in a quasiperiodic system the IDOS takes a value equal to the wave number of one of the Fourier components of the modulation potential.^{24,25}

Now, from a physical perspective the fragmentation scheme of the frequency spectrum can be interpreted in terms of resonant coupling effects involving an appropriate set of normal modes. In fact, in the light of previous works,^{26,27} the original Fibonacci chain will be decomposed into a series of *trimers* and *tetramers* of the form BAB and $BAAB$. The number of trimers present in the chain, n_{BAB} , equals the number of isolated A atoms. Analogously, the number of tetramers coincides with the number of AA pairs. Then, in the thermodynamic limit we have the well-known limits $\lim(n_{BAB}/N)=\tau^4$ and $\lim(n_{BAAB}/N)=\tau^3$.

Now, neglecting the trivial translation modes $\lambda_0=0$, each trimer, if considered as an independent dynamical system, contributes with two different normal vibration modes, whose respective frequencies are given by

$$\lambda_b = \alpha^{-1}, \quad \lambda_d = 2 + \alpha^{-1}, \quad (4a)$$

and, analogously, each tetramer contributes with three different normal modes given by

$$\lambda_c = 1 + \alpha^{-1}, \quad \lambda_{e,a} = \gamma + \eta \pm \sqrt{(\eta - \gamma)^2 + 2\gamma}, \quad (4b)$$

where $\eta \equiv (1 + \alpha^{-1})/2$. Hence, we have *five* normal modes describing the *fundamental* dynamical state of the FQC. If we assume that these normal modes are resonantly coupled in a way analogous to that discussed in the study of the electronic problem,^{26,27} we can assign the origin of every main subband appearing in the frequency spectrum to a specific normal mode belonging to the set given by the expressions (4). Such a procedure is illustrated in Fig. 3 and we realize that the lower-frequency region of the spectrum ($\lambda < 1$) contains two main contributions: the lowest-frequency contribution ($\lambda \leq 0.5$), which is related to the tetramers normal mode λ_a (contributing with τ^3 states), and the frequency interval $0.5 \leq \lambda \leq 1$, which is related to the trimers normal mode λ_b (contributing with τ^4 states). Therefore, although

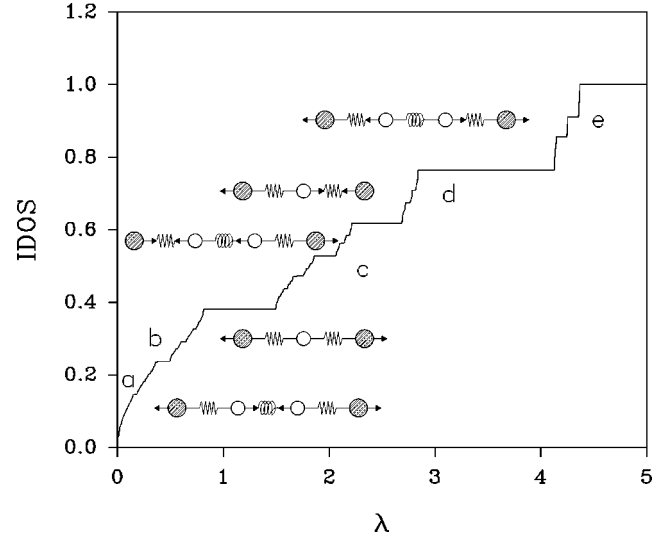


FIG. 3. Correspondence between the main subbands in the frequency spectrum of a Fibonacci quasicrystal with $N=610$, $\alpha=2$, and $\gamma=2$, and the normal modes associated with the trimers and tetramers introduced in our renormalization scheme.

both subbands are separated by a quite narrow gap, their origin can be traced back to the dynamics of quite different vibrating blocks in the FQC.

IV. NATURE OF THE PHONON STATES

From a mathematical point of view the nature of a state is determined by the measure of the spectrum to which it belongs. Consequently, since it has been proved that Fibonacci lattices have purely singular continuous spectra,²² we can properly state that all the states are critical in these systems. However, this fact does not necessarily imply that all these critical states behave in exactly the same way from a physical viewpoint. In fact, the possible existence of *critical extended* states in several kinds of aperiodic systems, including both quasiperiodic²⁸⁻³¹ and nonquasiperiodic ones,³² has been discussed in the last few years, spurring interest in the precise nature of critical wave functions and their role in the physics of aperiodic systems.³³

From a physical viewpoint, states can be classified according to their *transport properties*. Thus, conducting states in crystalline systems are described by periodic Bloch states, whereas insulating systems exhibit exponentially decaying wave functions corresponding to localized states. In this sense, since the amplitudes of critical states in a Fibonacci lattice do not tend to zero at infinity, but are bounded below throughout the system,³⁴ one may expect their physical behavior to be more similar to that corresponding to extended states than to localized ones. In fact, in the case of the electron dynamics, we have shown that critical states belonging to a subset of the spectrum of a general Fibonacci chain are extended from a physical point of view.³⁵

In this section we will study the transport properties of phonon states belonging to the frequency spectrum of the FQC as measured by their related transmission coefficients. Our approach³⁵⁻³⁷ is based on the transfer-matrix technique, where the dynamical equation (1) is described by the following transfer matrices:

$$\begin{aligned}
X &\equiv \begin{pmatrix} 2-\alpha\lambda & -1 \\ 1 & 0 \end{pmatrix}, & Y &\equiv \begin{pmatrix} 1+\gamma^{-1}(1-\lambda) & -\gamma^{-1} \\ 1 & 0 \end{pmatrix}, \\
Z &\equiv \begin{pmatrix} 1+\gamma-\lambda & -\gamma \\ 1 & 0 \end{pmatrix}, & W &\equiv \begin{pmatrix} 2-\lambda & -1 \\ 1 & 0 \end{pmatrix}. \quad (5)
\end{aligned}$$

The key point of our procedure consists in the fact that we renormalize the entire set of transfer matrices instead of the lattice itself. Making use of these matrices, and imposing cyclic boundary conditions, we can *translate* the atomic sequence $ABAAB\dots$ describing the topological order of the FQC to the transfer-matrix sequence $XZYXZYXWXZYXW\dots$ describing the phonon dynamics. By renormalizing this transfer-matrix sequence according to the blocking scheme $R_A \equiv ZYX$ and $R_B \equiv WX$, we get the considerably simplified sequence $R_B R_A R_A R_B R_A \dots$. The renormalized transfer-matrix sequence is also arranged according to the Fibonacci sequence and, consequently, *the topological order present in the original FQC is preserved by the renormalization process*. The R matrices are *unimodular* (i.e., their determinant equals unity) and they commute for certain frequency values. In fact, after some algebra we get

$$[R_A, R_B] = \frac{\lambda}{\gamma} \{2\gamma - 1 - \alpha[1 + \lambda(\gamma - 1)]\} \begin{pmatrix} 1 & 0 \\ 2 - \alpha\lambda & -1 \end{pmatrix}, \quad (6)$$

which vanishes for the frequencies given by the expression

$$\lambda^* = \frac{\alpha - 2\gamma + 1}{\alpha(1 - \gamma)}. \quad (7)$$

For these frequencies the global transfer matrix of the system, $M(N) \equiv R_A^{n_A} R_B^{n_B}$, with $n_A \equiv F_{n-3}$ and $n_B \equiv F_{n-4}$, can be explicitly evaluated in terms of Chebyshev polynomials of the second kind.³⁸ In this way, given any arbitrary FQC, we are able to obtain a subset of its frequency spectrum whose eigenstates can be analytically studied. A detailed study of the critical normal modes corresponding to the particular case $\gamma = 1/2$ has been recently discussed.³⁹ In this case the commutation frequency becomes independent of the values assigned to the mass distribution in the FQC. If we choose the values for the masses in such a way that their ratio satisfies the relationship $\alpha = F_{n-1}/F_{n-2}$, we get a *transparent* state with $t = 1$. Nonetheless, the power spectrum of this extended critical normal mode reveals that it *still preserves a significant degree of quasiperiodic order* in its inner structure.

Another set of interesting particular cases is obtained when the resonance frequency given by expression (7) coincides with some of the normal modes of the different trimers or tetramers given by expressions (4). The resonance conditions we are interested in are satisfied by those FQCs whose parameters verify one of the following relationships:

$$\alpha = \gamma \quad (\lambda^* = \lambda_b), \quad (8a)$$

$$\alpha = \frac{\gamma}{2\gamma - 1} \quad (\lambda^* = \lambda_d), \quad (8b)$$

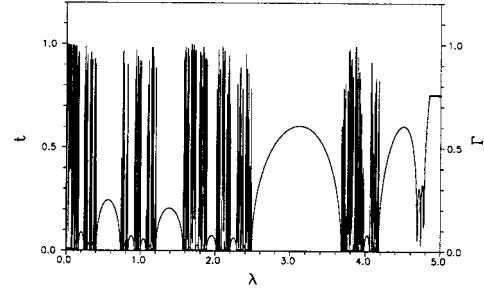


FIG. 4. Overall structure of the frequency spectrum for a Fibonacci quasicrystal with $N=610$, and $\alpha = \gamma = \sqrt{3}/3$, as given by the transmission and Lyapunov coefficients.

$$\alpha = \frac{\gamma^2 \pm (\gamma - 1)\sqrt{\gamma^2 + 2\gamma - 1}}{2\gamma - 1} \quad (\lambda^* = \lambda_{e,a}), \quad (8c)$$

with $\gamma \neq 1/2$. The condition $\lambda^* = \lambda_c$ can only be fulfilled in the trivial periodic case $\alpha = 1$. As a suitable illustrative example, in Fig. 4 we show the overall structure of the frequency spectrum for a FQC with $N=610$ and $\alpha = \gamma = \sqrt{3}/3$ in terms of the transmission and Lyapunov coefficients. By inspecting this figure one can realize that a significant fraction of the allowed states exhibit high values of the transmission coefficient. In addition, the presence of these states is not restricted, as is usual, to the lower-frequency region of the spectrum ($\lambda \leq 1$), but they are also present in the intermediate- ($1 \leq \lambda \leq 2.5$) and even at the high-frequency ($\lambda \approx 4$) regions. Let us consider the case $\lambda^* = \lambda_b = \sqrt{3}$ in more detail. According to the Cayley-Hamilton theorem, we can express the global transfer matrix in the closed form

$$M(N, \lambda^*) = \begin{pmatrix} \cos \phi + q \sin \phi & -2q \sin \phi \\ -2 \sin \phi & \cos \phi - q \sin \phi \end{pmatrix}, \quad (9)$$

where $q \equiv \sqrt{3} - 2$ and $\phi(N) \equiv (N - 7n_B)\pi/6$, and plugging the matrix coefficients given in Eq. (9) into Eq. (2) we obtain

$$t(N, \lambda^*) = \frac{1}{1 + 8(16 - 9\sqrt{3})\sin^2 \phi(N)}. \quad (10)$$

Several conclusions can be drawn from expression (10). First, we observe that the transmission coefficient remains always bounded below for *any* value of the lattice length, a fact which proves the extended nature of the corresponding state in the quasiperiodic limit. Second, we can make use of expression (10) to evaluate the transmission coefficient for different lattice lengths. The obtained results are summarized in Table I. By inspecting this table it can be readily noticed that the transmission coefficient (i) can only take on four different possible values, (ii) these values repeat according to a 12-fold period, and (iii) it is possible to find FQCs able to support states satisfying the transparency condition $t = 1$. To this end the system length should satisfy the condition $\sin^2 \phi(N) = 0$, which implies $N = 7n_B + 6l$, l being an arbitrary integer. It can be rigorously proved that Fibonacci systems satisfying that condition are determined by the sequence $N = F_{7+12k}$, with $k = 0, 1, \dots$.⁴⁰

In this way, we realize that the transport properties of a normal mode vibrating at the resonance frequency $\lambda^* = \sqrt{3}$

TABLE I. Dependence of the transmission coefficient of the resonant state $\lambda^* = \sqrt{3}$ with the lattice length for a Fibonacci quasicrystal with $\alpha = \gamma = \sqrt{3}/3$.

n	$N = F_n$	$n_B = F_{n-4}$	$t(N, \lambda^*)$
5	8	1	0.5485 ...
6	13	2	0.5485 ...
7	21	3	1.0000
8	34	5	0.5485 ...
9	55	8	0.5485 ...
10	89	13	0.2882 ...
11	144	21	0.2329 ...
12	233	34	0.5485 ...
13	377	55	0.2882 ...
14	610	89	0.5485 ...
15	987	144	0.2329 ...
16	1597	233	0.2882 ...
17	2584	377	0.5485 ...
18	4181	610	0.5485 ...
19	6765	987	1.0000
20	10946	1597	0.5485 ...

significantly depend on the lattice length. In fact, the value of its transmission coefficient *oscillates periodically* between the extreme values $t_{max} = 1$ and $t_{min} = 0.23297 \dots$. A family of states exhibiting a similar behavior has been recently found in the electronic energy spectra of Koch fractal lattices.³⁶ In that work these kinds of states were tentatively referred to as *almost transparent* ones, and it was argued that their related transport properties may be more similar to those corresponding to the usual transparent states than to localized ones. The finding of analogous states in the frequency spectra of the FQCs considered in this work provides another example of the richness and diversity of the physical behaviors associated with critical states in aperiodic systems.

V. THERMAL CONDUCTIVITY

Heat transport can be described in terms of the phenomenological relationship (Fourier's law)

$$J = -\kappa \nabla T, \quad (11)$$

where J is the heat flow, κ is the thermal conductivity, and ∇T is the temperature gradient. The question as to whether the heat conduction of a one-dimensional system obeys Fourier's heat law is yet an open problem. As a general appreciation, it can be said that the validity of Fourier's law cannot be guaranteed *a priori*, although it accurately describes the thermal behavior of certain particular systems.⁴¹ Thus, it has been reported that the heat conduction through a Fibonacci-Toda lattice obeys Fourier's law.⁴² Consequently, we will assume, as a suitable working hypothesis, that Fourier's law provides an adequate phenomenological description of heat transfer in FQCs.

A. Contribution of the different modes

In order to ascertain the influence of the fragmented nature of the phonon spectrum on the thermal transport prop-

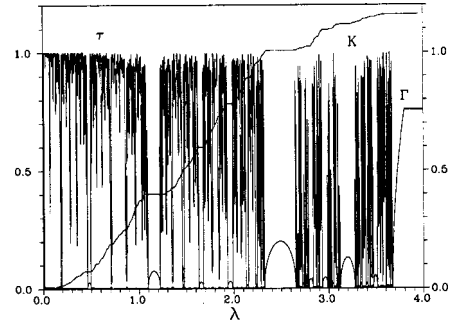


FIG. 5. Comparison between the thermal coefficient \mathcal{K} and the overall structure of the frequency spectrum for a Fibonacci quasicrystal with $N = 610$, $\alpha = 1.2$, and $\gamma = 0.9$ as given by the transmission and the Lyapunov coefficients. The \mathcal{K} curve is given in arbitrary units, and it has been properly scaled to make the comparison with the other magnitudes easier.

erties of FQCs, in this section we shall study the thermal conductivity by considering the contribution of the different modes to the energy transport. To this end, we will consider the lattice in thermal contact with two reservoirs at different temperatures T_1 and T_N ($T_N > T_1$). The thermal flow through the lattice can be described by means of the expression⁴³

$$J = -c(T_N - T_1)\mathcal{K}, \quad (12a)$$

where $c \ll 1$ is an appropriate factor measuring the time interval between collisions at the reservoirs (effective viscosity), and

$$\mathcal{K} \equiv \sum_{\nu} (\xi_{\nu,1}^{-2} + \xi_{\nu,N}^{-2})^{-1}, \quad (12b)$$

where $\xi_{\nu,n} \equiv \sqrt{m_n} u_{\nu,n}$, and $u_{\nu,1}$ and $u_{\nu,N}$ are the amplitudes of the ν th mode at the lattice ends. By comparing expressions (11) and (12) we observe that the coefficient \mathcal{K} is proportional to κ , and provides us with pertinent information about the contribution of each vibration mode to the thermal conductivity value. The applicability of expression (12b) to the study of the lattice thermal transport in *periodic* one-dimensional chains has been recently reviewed by Frizzera *et al.*,⁴⁴ concluding that both low- and high-frequency modes do not appreciably contribute to the thermal transport.

Our results for the *quasiperiodic* FQC are presented in Fig. 5, where we compare the behavior of the thermal coefficient \mathcal{K} with the overall structure of the phonon frequency spectrum. The curve for \mathcal{K} displays the cumulative contributions to the thermal conductivity as a function of the mode frequency and exhibits a series of steps separated by well-defined plateaus, corresponding to the main gaps of the phonon spectrum. The slope of the steps is determined by the successive contributions of the different modes comprised within the corresponding allowed subbands. In this way, we realize that the fragmented nature of the frequency spectrum is reflected by the stepped behavior of the thermal coefficient. In addition, we observe that the main contribution to the final value of the thermal coefficient is provided by the modes comprised in the intervals $0.5 < \lambda < 1.1$ and $1.2 < \lambda < 2.3$; meanwhile the contribution due to both lower ($\lambda < 0.5$) and higher ($\lambda > 2.6$) frequencies is only a subsidiary

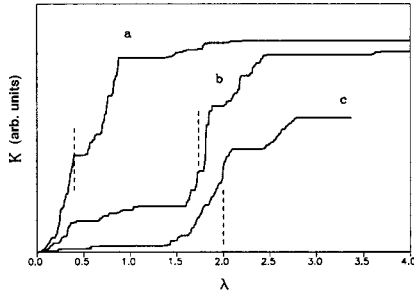


FIG. 6. Comparison among the thermal coefficients \mathcal{K} corresponding to different Fibonacci quasicrystals with $N=1597$ and (a) $\alpha = \sqrt{3}$, $\gamma = 1 + \sqrt{3}/3$ ($\lambda^* = \lambda_a = 1 - \sqrt{3}/3$); (b) $\alpha = \gamma = \sqrt{3}/3$ ($\lambda^* = \lambda_b = \sqrt{3}$); and (c) $\alpha = 1.2$, $\gamma = 0.5$, and $\lambda^* = 2$. The curves are given in arbitrary units and they have been properly scaled to facilitate the comparison. The vertical dashed lines indicate the values of the different resonance frequencies.

one, in qualitative agreement with the general behavior previously purported for periodic systems.⁴⁴ In our quasiperiodic case, the significant level off of the \mathcal{K} curve for high-frequency modes clearly indicates that these modes should not play a significant role in the thermal transport of FQCs, even if one takes into account the relatively high values of their related transmission coefficients, as reported in Fig. 5.

We shall now consider the behavior of the thermal coefficient under the resonance conditions discussed in the previous section. Such a behavior is illustrated in Fig. 6 for three different FQCs, exhibiting the resonance frequencies $\lambda^* = 2$, $\lambda^* = \lambda_a = 1 - \sqrt{3}/3$, and $\lambda^* = \lambda_b = \sqrt{3}$, respectively. The overall stepped structure of the curves is similar to that shown for a typical FQC in Fig. 5. However, a closer inspection reveals that the \mathcal{K} curve significantly grows and steepens around the values corresponding to the resonance frequencies (vertical dashed lines in Fig. 6). This feature indicates that, under resonance conditions, the value of the thermal flow through the lattice is significantly influenced by the normal vibration modes located around the resonance frequencies λ^* .

B. Finite-temperature effects

In order to obtain realistic outcomes from the model it is convenient to include finite-temperature effects. To this end, we will make use of the following expression for the thermal conductivity (expressed in k_B^2/\hbar units):⁴⁵

$$\kappa(N, T) = \frac{1}{2\pi T} \times \frac{\int_0^{\omega^*} \left(-\frac{\partial n}{\partial \omega} \right) \omega^2 d\omega \int_0^{\omega^*} \left(-\frac{\partial n}{\partial \omega} \right) \omega^2 t(N, \omega) d\omega}{\int_0^{\omega^*} \left(-\frac{\partial n}{\partial \omega} \right) [1 - t(N, \omega)] \omega^2 d\omega}, \quad (13)$$

where k_B is the Boltzmann constant, ω^* is a threshold frequency related to the Debye temperature as $\Theta = \hbar \omega^*/k_B$, $n(\omega, T)$ is the Bose-Einstein distribution, and $t(N, \omega)$ is the transmission coefficient.

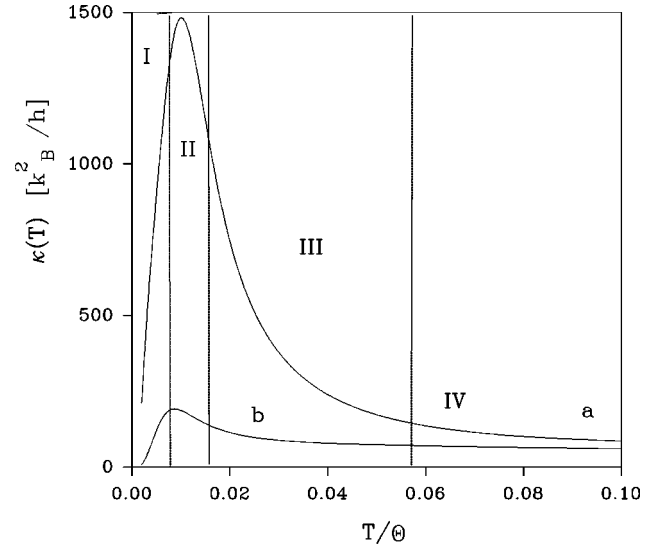


FIG. 7. Temperature dependence of the thermal conductivity in Fibonacci quasilattices with $N=987$ atoms corresponding to (a) the on-site model with $\alpha = 1.2$, $\gamma = 1.0$ and (b) our general model with $\alpha = 1.2$, and $\gamma = 0.9$.

Making use of Eq. (13) we have obtained the temperature dependence of the thermal conductivity by numerical integration. In Fig. 7 we compare the thermal conductivity for two kinds of Fibonacci quasilattices. In both cases we appreciate a similar behavior, defining four different temperature ranges: a low-temperature region (I) characterized by a steeped increase of κ with T and a well-defined thermal conductivity maximum in region II, followed by a marked decrease in thermal conductivity in the intermediate temperature region (III), which tends to an asymptotic behavior in the high-temperature limit (IV). We also note that the overall thermal conductivity (as measured by the area under the corresponding curve) is significantly higher for the simplest on-site model than for the more realistic FQC. This result is in line with the purported low thermal conductivity observed in quasicrystalline samples.

It is worthwhile to mention that the qualitative behavior of these curves is remarkably similar to that recently reported for some high-quality icosahedral, monograind QCs.^{6,7} However, this analogy should not be pushed too far. In fact, in crystalline specimens the characteristic low-temperature peak arises from the competition between the exponential decay of umklapp processes with decreasing temperature and the onset of boundary scattering at very low temperatures. Since none of these physical mechanisms have been explicitly included in our treatment, the behavior of the thermal conductivity curves shown in Fig. 7 should more properly be attributed to the fractal structure of the frequency spectrum.

C. Analytical expressions

In order to ascertain such a possibility analytically we will assume that, in the quasiperiodic limit ($N \gg 1$), the transmission coefficient can be roughly approximated by a *self-similar Dirac comb* given by the expression⁴⁶

$$t(N, \omega) \approx \sum_{i=1}^N \eta_i \delta(\omega - \omega_i), \quad (14)$$

where η_i measures the strength of the i th transmission peak and ω_i gives its position in the frequency spectrum. Making use of Eq. (14) in Eq. (13), and taking into account that in the quasiperiodic limit $1 - t(N, \omega) \approx 1$, we get

$$\kappa(T) \approx \frac{k_B}{h} \sum_{i=1}^{N'} f_{\omega_i}(u), \quad (15)$$

where we have explicitly assumed that only the modes associated with high values of the transmission coefficient ($\eta_i \rightarrow 1$) significantly contribute to the thermal conductivity (hence $N' < N$), and we have defined

$$f_{\omega_i}(u) \equiv \frac{u^2 \omega_i^2 e^{u \omega_i}}{(e^{u \omega_i} - 1)^2}, \quad (16)$$

with $u = \hbar/k_B T$. This expression is analogous to that previously obtained for the thermal coefficient \mathcal{K} , in the sense that it gives the thermal conductivity as a cumulative contribution which takes into account the different normal modes present in the lattice. At this point it is convenient to rearrange expression (15):

$$\kappa(T) = \frac{k_B}{h} \sum_{i=1}^{N'} \left(\frac{x_i}{\sinh x_i} \right)^2, \quad (17)$$

where $x_i \equiv (\Theta/T)(\omega_i/2\omega^*)$. Since the Debye temperatures of most QCs studied to date exhibit quite high values (in the range $400 \leq \Theta \leq 500$),^{47,48} we can confidently approximate expression (17) by its high-temperature limit expansion

$$\kappa(T) \approx \frac{\hbar}{2\pi k_B} \sum_{i=1}^{N'} \omega_i^2 g_{\omega_i}(T), \quad (18)$$

where we have introduced the auxiliary functions

$$g_{\omega_i}(T) \equiv T^{-2} e^{-\Theta \omega_i / T \omega^*}. \quad (19)$$

In this way, the variation of the thermal conductivity with the temperature is determined by the superposition of a series of functions given by expression (19). For a given value of the frequency ω_i , the behavior of each of these functions is completely analogous to that shown in Fig. 7, although the position of the maximum depends, in each case, on the frequency value according to the relationship $T_{max} = \Theta \omega_i / 2\omega^*$. Therefore, expression (18) allows us to precisely analyze the contribution of each normal mode present in the lattice to the thermal conductivity at a given temperature.

As an example, we shall consider the case corresponding to the resonance frequency $\lambda^* = 2$ ($\omega = \sqrt{2}$). In that case the most significant contribution to the thermal conductivity comes from those normal modes located around the resonance frequency (see Fig. 6). Therefore, we can confidently expect that the position of the thermal conductivity maximum will be mainly determined by the normal mode corresponding to the resonance frequency $\omega = \sqrt{2}$. By taking the derivative of expression (18), the position of the maximum can be estimated in terms of physical parameters of the system as

$$T_{max} \approx \frac{\sqrt{2} \hbar}{2k_B} \left(\frac{K_{AB}}{m_A} \right)^{1/2}. \quad (20)$$

Although this expression is just a rough approximation, by plugging the values $K_{AB} = 10^3 \text{ dyn cm}^{-1}$, and $m_A = 10^{-23} \text{ g}$ as representative ones, we get $T_{max} \approx 40 \text{ K}$. This figure compares well with the experimental values obtained for high-quality, monograind quasicrystalline samples.⁷

VI. CONCLUSIONS

In this work we have considered the thermal transport properties of FQCs, paying special attention to the possible influence of the singular nature of their phonon frequency spectrum on the thermal conductivity. With this goal in mind, we have studied in detail the physical mechanisms giving rise to the fractal structure of the frequency spectrum, providing a suitable explanation on the basis of resonant coupling effects among a fundamental set of normal modes.

Another interesting result of this work regards the relationship between the spatial distribution of the normal modes amplitudes and their related transport properties. The richness of the frequency spectrum associated with FQCs is illustrated by the existence of a great variety of critical normal modes, exhibiting quite different physical behaviors, which range from highly conducting extended states, satisfying the transparency condition $t=1$ for any value of N , to almost transparent states, whose transmission coefficient oscillates periodically between two extreme values depending on the system length.

With regard to the contribution of the different normal modes to the thermal transport through FQCs we can highlight the following results. In the first place, the highly fragmented structure of the frequency spectrum has a significant influence in the cumulative contribution of the different normal modes to the thermal transport. In the second place, we find that the value of the transmission coefficient alone should not be considered as a *definitive criterion* when determining the thermal transport efficiency of an arbitrary normal mode, as is conveniently illustrated by the presence of a set of normal modes exhibiting high transmission coefficient values (but a poorly conductive character) in the high-frequency region of the spectrum (see Figs. 2, 4, and 5). In the third place, the sudden enhancement of the thermal coefficient \mathcal{K} around the resonance frequencies clearly indicates the importance of the *collective resonant motion* determined by the fundamental normal modes associated with the set of trimers and tetramers introduced in Sec. III to the thermal conductivity of FQCs.

We have also introduced an analytical approach which allows us to properly describe the dependence of the $\kappa(T)$ curve on the temperature over a wide temperature range, as a superposition of different contributions associated with each normal mode present in the system at a given temperature. According to expression (18) all these contributions have a similar mathematical dependence with temperature, but their relative contribution to the final thermal conductivity of the FQC is weighed by the ω_i^2 factor. Since the number of allowed states available at a given temperature is prescribed by the fractal pattern of the frequency spectrum, expression (18) provides a clear physical picture of the way the self-similar

nature of the phonon spectrum influences the overall behavior of the thermal conductivity curve of FQCs over a wide temperature range.

To conclude we shall briefly consider the applicability of some of our results to decagonal (2D) and icosahedral (3D) quasicrystals. From a broad perspective, we can invoke some fundamental reasons supporting the use of one-dimensional models as a first approximation to the study of realistic quasicrystalline systems. In fact, in the light of Conway's theorem, both the fractal structure of the frequency spectra and the existence of critical states can be explained in terms of resonant coupling effects.^{49,50} Therefore, the physical mechanisms at work are not so dependent on the dimension of the system, but are mainly determined by the self-similarity of the underlying structure.¹⁰ Consequently, in order to ascertain whether some of the purported anomalies in the thermal transport properties of quasicrystals are directly related to the

kind of order present in their structure (a basic point for any general theory of quasicrystalline matter), the results obtained with our 1D model may be considered as quite representative, for such models encompass, in the simplest possible manner, most of the novel physics attributable to the quasiperiodic order.

ACKNOWLEDGMENTS

I gratefully thank Francisco Domínguez-Adame for his collaboration on these topics during these years. I also thank M. Victoria Hernández for her illuminating questions. I warmly thank Miguel Angel García for many interesting conversations on Fibonacci numbers. This work was supported by Universidad Complutense de Madrid through Project No. PR64/99-8510.

*Electronic address: macia@valbuena.fis.ucm.es

¹A.P. Tsai, A. Inoue, and T. Masumoto, *Jpn. J. Appl. Phys., Part 1* **27**, 1587 (1988); *Mater. Trans., JIM* **31**, 98 (1990).

²L.X. He, Y.K. Wu, and K.H. Kuo, *J. Mater. Sci. Lett.* **7**, 1284 (1988); A.P. Tsai, A. Inoue, and T. Masumoto, *Mater. Trans., JIM* **30**, 463 (1989).

³D. Shechtman, I. Blech, D. Gratias, and J.W. Cahn, *Phys. Rev. Lett.* **53**, 1951 (1984); D. Levine and P.J. Steinhardt, *ibid.* **53**, 2477 (1984).

⁴See, for example, S. Roche, G. Trambly de Laissardiére, and D. Mayou, *J. Math. Phys.* **38**, 1794 (1997) and references therein.

⁵J.M. Dubois, S.S. Kang, P. Archambault, and B. Colleret, *J. Mater. Res.* **8**, 38 (1993).

⁶M.A. Chernikov, A. Bianchi, and H.R. Ott, *Phys. Rev. B* **51**, 153 (1995).

⁷S. Legault, B. Eelman, J.O. Ström-Olsen, L. Taillefer, S. Kycia, T. Lograsso, and D. Delaney, in *New Horizons in Quasicrystals: Research and Applications*, edited by A.I. Goldman, D.J. Sordelet, P.A. Thiel, and J.M. Dubois (World Scientific, Singapore, 1997).

⁸M.A. Chernikov, E. Felder, A. Bianchi, C. Wälti, M. Kenzelmann, H.R. Ott, K. Edagawa, M. de Boissieu, C. Janot, M. Feuerbacher, N. Tamura, and K. Urban, in *Proceedings of the 6th International Conference on Quasicrystals*, edited by S. Takeuchi and T. Fujiwara (World Scientific, Singapore, 1998).

⁹J.W. Vandersande and C. Wood, *Contemp. Phys.* **27**, 117 (1986).

¹⁰P.A. Kalugin, M.A. Chernikov, A. Bianchi, and H.R. Ott, *Phys. Rev. B* **53**, 14 145 (1996).

¹¹N. Vernier, G. Bellessa, B. Perrin, A. Zarembowitch, and M. de Boissieu, *Europhys. Lett.* **22**, 187 (1993).

¹²C. Janot, *Phys. Rev. B* **53**, 181 (1996).

¹³R.K. Pattnaik and E.A. Whittaker, *J. Phys. A* **25**, 577 (1992).

¹⁴C. Tsallis, L.R. da Silva, R.S. Mendes, R.O. Vallejos, and A.M. Mariz, *Phys. Rev. E* **56**, R4922 (1997); R.O. Vallejos, R.S. Mendes, L.R. da Silva, and C. Tsallis, *ibid.* **58**, 1346 (1998).

¹⁵J. Lu, T. Odagaki, and J.L. Birman, *Phys. Rev. B* **33**, 4809 (1986); F. Nori and J. F. Rodriguez, *ibid.* **34**, 2207 (1986).

¹⁶K. Machida and M. Fujita, *J. Phys. Soc. Jpn.* **55**, 1799 (1986).

¹⁷M. Kohmoto and J.R. Banavar, *Phys. Rev. B* **34**, 563 (1986).

¹⁸Y. Liu and R. Riklund, *Phys. Rev. B* **35**, 6034 (1987).

¹⁹D. Würtz, T. Schneider, and A. Politi, *Phys. Lett. A* **129**, 88 (1988).

²⁰J.A. Ashraff and R.B. Stinchcombe, *Phys. Rev. B* **37**, 5723 (1988).

²¹A. Chakrabarti, S.N. Karmakar, and R.K. Moitra, *J. Phys.: Condens. Matter* **1**, 1017 (1989); A. Ghosh and S.N. Karmakar, *Phys. Rev. B* **57**, 2834 (1998).

²²A. Süto, *J. Stat. Phys.* **56**, 525 (1989); J. Bellissard, B. Iochum, E. Scoppola, and D. Testard, *Commun. Math. Phys.* **125**, 527 (1989).

²³P. Dean, *Rev. Mod. Phys.* **44**, 127 (1972).

²⁴J. Bellissard, B. Iochum, and D. Testard, *Commun. Math. Phys.* **141**, 353 (1991); J. Bellissard, A. Bovier, and J.M. Ghez, *Rev. Math. Phys.* **4**, 1 (1992).

²⁵J.M. Luck, *Phys. Rev. B* **39**, 5834 (1989).

²⁶Q. Niu and F. Nori, *Phys. Rev. Lett.* **57**, 2057 (1986); Q. Niu and F. Nori, *Phys. Rev. B* **42**, 10 329 (1990); Y. Liu and W. Sritrakool, *ibid.* **43**, 1110 (1991).

²⁷E. Maciá, F. Domínguez-Adame, and A. Sánchez, *Phys. Rev. E* **50**, 679 (1994).

²⁸V. Kumar and G. Ananthakrishna, *Phys. Rev. Lett.* **59**, 1476 (1987).

²⁹X.C. Xie and S. Das Sarma, *Phys. Rev. Lett.* **60**, 1585 (1988); G. Ananthakrishna and V. Kumar, *ibid.* **60**, 1586 (1988).

³⁰V. Kumar, *J. Phys.: Condens. Matter* **2**, 1349 (1990).

³¹A. Chakrabarti, S.N. Karmakar, and R.K. Moitra, *Phys. Lett. A* **168**, 301 (1992); G.Y. Oh, C.S. Ryu, and M.H. Lee, *J. Phys.: Condens. Matter* **4**, 8187 (1992); A. Chakrabarti, S.N. Karmakar, and R.K. Moitra, *Phys. Rev. B* **50**, 13 276 (1994).

³²M. Severin, M. Dulea, and R. Riklund, *J. Phys.: Condens. Matter* **1**, 8851 (1989); S. Sil, S.N. Karmakar, R.K. Moitra, and A. Chakrabarti, *Phys. Rev. B* **48**, 4192 (1993).

³³E. Maciá and F. Domínguez-Adame, *Phys. Rev. B* **50**, 16 856 (1994); F. Domínguez-Adame, E. Maciá, and A. Sánchez, *ibid.* **51**, 878 (1995).

³⁴B. Iochum and D. Testard, *J. Stat. Phys.* **65**, 715 (1991).

³⁵E. Maciá and F. Domínguez-Adame, *Phys. Rev. Lett.* **76**, 2957 (1996).

³⁶E. Maciá, *Phys. Rev. B* **57**, 7661 (1998).

³⁷E. Maciá and F. Domínguez-Adame, in *Proceedings of the International Conference on Aperiodic Crystals*, edited by M. de Boissieu, R. Currat, and J.-L. Verger-Gaugry (World Scientific, Singapore, 1998).

³⁸See, for example, J. M. Luck, *Fundamental Problems in Statisti-*

- cal Mechanics VIII* (Elsevier, New York, 1994).
- ³⁹E. Maciá, Phys. Rev. B **60**, 10 032 (1999).
- ⁴⁰E. Maciá, Mater. Sci. Eng. A (to be published). I am indebted to Miguel Angel García for the proof.
- ⁴¹T. Hatano, Phys. Rev. E **59**, R1 (1999); E.A. Jackson and A.D. Mistriotis, J. Phys.: Condens. Matter **1**, 1223 (1989); F. Mokross and H. Büttner, J. Phys. C **16**, 4539 (1983).
- ⁴²N. Nishiguchi, N. Takahashi, and T. Sakuma, J. Phys.: Condens. Matter **4**, 1465 (1992).
- ⁴³H. Matsuda and K. Ishii, Prog. Theor. Phys. **45**, 51 (1970); W.M. Visscher, *ibid.* **46**, 729 (1971).
- ⁴⁴W. Frizzera, G. Viliani, M. Montagna, A. Monteil, and J.A. Capobianco, J. Phys.: Condens. Matter **9**, 10 867 (1997).
- ⁴⁵I.M. Lifshits, S.A. Gredeskul, and L.A. Pastur, *Introduction to the Theory of Disordered Systems* (Wiley, New York, 1988); H.L. Engquist and P.W. Anderson, Phys. Rev. B **24**, 1151 (1981).
- ⁴⁶E. Maciá, F. Domínguez-Adame, and A. Sánchez, Phys. Rev. B **49**, 9503 (1994).
- ⁴⁷J.L. Wagner, K.M. Wong, and S.J. Poon, Phys. Rev. B **39**, 8091 (1989).
- ⁴⁸D. Zhang, S. Cao, Y. Wang, L. Lu, X. Wang, X.L. Ma, and K.H. Kuo, Phys. Rev. Lett. **66**, 2778 (1991).
- ⁴⁹C. Sire, in *Proceedings of the 5th International Conference on Quasicrystals*, edited by C. Janot and R. Mosseri (World Scientific, Singapore, 1995).
- ⁵⁰J. Hafner, M. Krajčí, and M. Mihalkovič, Phys. Rev. Lett. **76**, 2738 (1996).